






## Analytical and Experimental Study of the Solidification of a Water in the Horizontal Moisturized Porous Slabs

Jacek Partyka<sup>1\*</sup>, Zygmunt Lipnicki<sup>2</sup>, Tomasz Małolepszy<sup>3</sup>

<sup>1</sup> Military Institute of Engineer Technology, Wrocław 50-961, Poland

<sup>2</sup> Institute of Environmental Engineering, University of Zielona Góra, Zielona Góra 65-516, Poland

<sup>3</sup> Institute of Mathematics, University of Zielona Góra, Zielona Góra 65-516, Poland

Corresponding Author Email: [partyka@witi.wroc.pl](mailto:partyka@witi.wroc.pl)

Copyright: ©2024 The authors. This article is published by IETA and is licensed under the CC BY 4.0 license (<http://creativecommons.org/licenses/by/4.0/>).

<https://doi.org/10.18280/ijht.420116>

### ABSTRACT

**Received:** 25 May 2023

**Revised:** 22 November 2023

**Accepted:** 8 January 2024

**Available online:** 29 February 2024

#### **Keywords:**

*horizontal fluid-saturated porous granular bed, free convection, solidification front, solidified layer*

The aim of the work is to develop a new analytical model of liquid solidification taking into account the phenomenon of free convection in horizontal, fluid-saturated, granular porous plates and to experimentally verify the theory. This model is based on previous theoretical research and experiments of the authors of this work. In order to determine the solidification front, the measuring cylinder method was used, in which the solidification front was determined indirectly by measuring the increase in water volume in a measuring cylinder connected to the test chamber. Based on the analysis of the phenomenon of free convection of water in a porous medium saturated with fluid, the heat transfer coefficient on the solidification surface was determined, which is an important parameter from the point of view of heat transfer. It was also deemed necessary to take into account the anomalous properties of water. The results of theoretical research were compared with the authors' experimental research and presented in pictorial form. Due to the great practical importance of the issue of freezing of the ground and elements of buildings and structures, it is necessary to understand this phenomenon as undesirable for the durability of building structures.

## 1. INTRODUCTION

Porous materials are often found in structural elements of buildings and they are exposed to the effects of negative temperatures in combination with the presence of water within them. The analysis of the solidification process of porous materials under low-temperature conditions is very important from a scientific and practical point of view, as it may affect the internal structure of the materials and cause deterioration of their functional properties. Consequently, freezing water in a fluid-saturated porous material can gravely damage the material, or even destroy it.

The problem of solidification of fluid-saturated porous media has been investigated by a number of authors [1-24], due to the complex and interesting nature of the phenomenon on one hand and research interest in the issue of the solidification within fluid-saturated porous media.

In turn, Partyka and Lipnicki [25] presents a simplified theoretical model of solidification of a water-saturated porous layer which was being cooled and where an experiment was carried out under laboratory conditions. On one side the layer was limited by a cold planar metal slab whose constant temperature was lower than the freezing point of water, and on the other, the layer's exterior surface was kept at a constant, room temperature. In that study, the heat transfer coefficient at the solidification front of the saturated porous medium was determined by analysing the phenomenon of free convection

in a water-saturated porous medium.

The theoretical model in the cited work simplified the actual phenomenon by not taking into account the cooling of the tested porous layer, while the presented experimental studies included measurements of the thickness of the solidified layer in a porous medium via studying the change (increase) in the volume of water in a measuring cylinder. Wang and Bejan [26] devoted their studies to defining the conditions for the formation of free convection and heat exchange in the fluid-saturated horizontal porous layer, however, they did not investigate the impact of the water anomaly phenomenon on the process of free convection.

Seki et al. [27] and Yen [28] of the works investigated the influence of water anomalies on the formation of free convection in its separated areas. The monography reviews theoretical and experimental works on the phenomenon of the formation of free water convection near the temperature of  $\sim 277\text{ K}$  in various geometric systems [28].

For porous materials, the solidification phenomenon also occurs in latent heat storage (LHS) media manufactured out of phase-change materials (PCM) filled with spheres, especially made of metal [29-32].

As is known, PCMs are usually bad heat conductors, and embedding metal spheres in them increases the effective thermal conductivity of the porous medium as a whole, as metal spheres are good heat conductors. Kenisarin et al. [33] points to a great need to conduct research on phase

transformations of porous PCMs, due to the latent heat storage problem being a serious issue in the power industry.

Considering the above, it is easy to see that there is a demand to carry on studies on the solidification of fluid-saturated porous materials, as they are important both in nature and in various technologies, with particular emphasis on their notable role in the construction and environmental engineering.

The aim of the work is to conduct a theoretical analysis of the solidification of horizontal, fluid-saturated, granular porous plates and to verify the theory with research experiments. Through theoretical analysis and experimental research, the authors of the work intend to advance scientific knowledge in the field of the impact of freezing water in the pores of humid porous media, and in particular by determining parameters related to the solidification process, such as the heat transfer coefficient at the solidification front, the thickness of the solidified layer in the research experiment, and the temperature in the porous medium. Solidification tests were performed on an original test stand, designed and constructed on the basis of an individual project. However, the thickness of the solidified layer was determined by the graduated cylinder method, which is a method for its appointment.

## 2. SELECTED PROPERTIES OF POROUS GRANULAR MEDIA

The mechanics of fluid-saturated granular porous materials is the subject of several intensive studies, and the obtained results could be used in numerous ways. Among others, the findings can be utilized in road construction, and the construction of structural layers of different thicknesses and variable grain sizes in particular. Granular porous beds can serve as constituents of concrete mixtures for varying applications.

Sobieski et al. [34] and Xu et al. [35] investigated a loose porous granular medium with a large free space, which ensured good water filtration thanks to differently shaped, loosely arranged solid particles. The internal structure of the space between granular porous media exerts a great influence on the course of various processes and phenomena occurring in porous materials themselves, and parameterization of these processes, as well as in-depth studies, are of immense scientific and practical importance. As porosity is a key quality characterizing granular porous media and has a notable impact on the properties of many materials, its experimental determination is one of the fundamental tests performed with porous materials [34]. Apart from porosity, an important parameter characterizing a given porous medium in terms of its ability to conduct heat is effective thermal conductivity, which is a parameter derived from porosity.

The porous medium analysed in this study is composed of a solid body, the matrix, which is an aggregate, with its pores/space between grains being filled with water or ice, should the water solidify. The thermal conductivity of a porous medium has the form of functional dependencies on the individual thermal conductivities of the components of the porous medium and on their volume shares for the assumed type of configuration of the discontinuous component - a solid body, in a continuous liquid matrix and in the form of the maximum value of effective conductivity. The equation that can be used to calculate the effective values of other parameters as well assumes the form [36]:

$$\Pi_{ef} = \varphi \Pi_{ice\ or\ water} + (1 - \varphi) \Pi_{solid\ particel}, \quad (1)$$

where,  $\Pi$ , apart from thermal conductivity, also expresses other parameters, such as specific heat, density, heat diffusion in the porous material and  $\varphi$  – porosity of the medium. It is worth adding that Eq. (1) is of great importance in determining the thermal conductivity of wet porous media, especially as in this work, when the porous medium is two-component, because it contains a solid body in the form of an aggregate and water.

This porosity is related to the material's susceptibility to absorbing fluids, and then to its ability to freeze under low temperatures [37-39]. In the above-mentioned research papers, the freezing of model porous materials relative to moisture migration was studied both theoretically and experimentally.

The analysis of the solidification process occurring in moist horizontal porous plates is very important from a theoretical point of view. In order to enable a theoretical solution of the problem, it was introduced for consideration, a simplified theoretical model in which the assumptions and conditions adopted allow numerical calculations to be performed later in the work.

## 3. THEORETICAL MODEL OF A FLUID – SATURATED POROUS SLAB

### 3.1 Problem formulation

The theoretical solution of the problem involved a simplified theoretical model being introduced, in which the assumptions and the set conditions yielded solutions and allowed the authors to perform numerical calculations. For the modelling of the solidification process of a planar fluid-saturated porous layer, two variants were adopted depending on their orientation. These are presented in Figure 1.

Figure 1 shows two cases, where porous (granular) and fluid-saturated planar slabs with porosity  $\varphi$  and thickness  $H$  are positioned in two ways with respect to the gravitational acceleration  $\vec{g}$ . The slab is thermally insulated on one side, while on the other, it is cooled by means of a heat flux  $q$ , flowing into the environment characterised by constant air temperature  $T_{en}$  which is lower than the freezing point of water:  $T_{en} < T_F$ . The slab solidifies on the non-insulated side, whose outer surface temperature equals  $T_w$ . As a result of the movement of the solidification front of the liquid with a temperature  $T_F$ , a solidified layer is formed, whose thickness equals  $\delta$ . In both cases, the slab positioning illustrates the sub-areas (convection cells) in which free convection may or may not occur.

The boundary of the sub-areas is determined by the temperature of the water anomaly  $T_a$  and the position of this isothermal plane is determined by the height  $\vec{H}$ . In the sub-areas where free convection may potentially occur, convective Bénard cells with a  $l$  and height equal  $\vec{H} - \delta$  (case “a”) and  $H - \vec{H} - \delta$  (case “b”) were marked. In the remaining sub-areas, only heat transfer occurs. The free convection sub-areas shown in Figure 1 are the result of the temperature distributions, which are necessary but insufficient conditions for the occurrence of free convection. In a porous medium, these conditions will be governed by the magnitude of the Rayleigh number, the value of which should exceed the critical Rayleigh number  $-Ra > Ra_c$ .

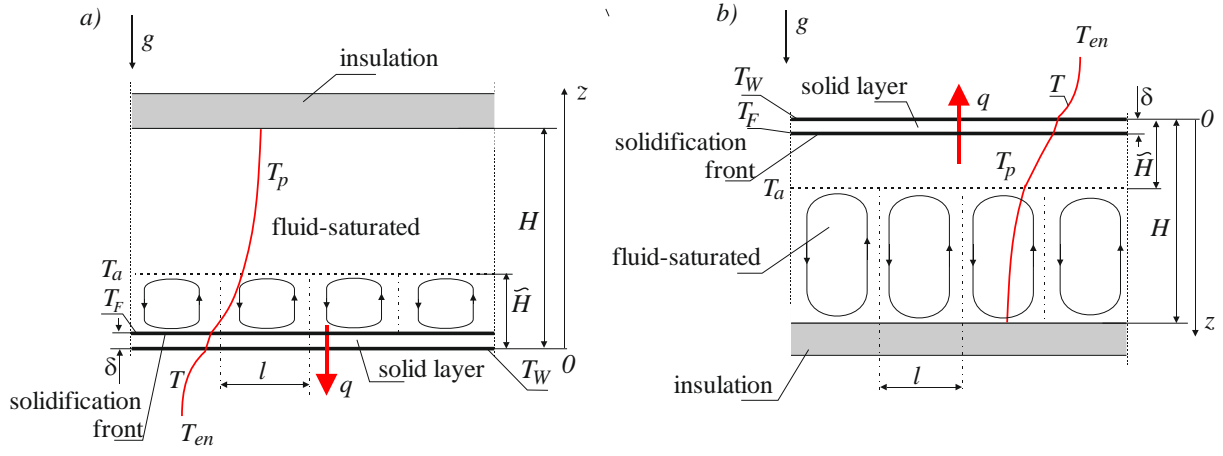


**Figure 1.** Variants of solidification of a planar fluid-saturated porous layer as dependent on its position

In both cases, the heat balance for the growing solidified layer is described by the quasi-stationary one-dimensional equation:

$$h_F(T_p - T_F) + \varphi \rho_S L \frac{d\delta}{dt} = \frac{k_{sp}}{\delta} (T_F - T_W) = h_{en}(T_W - T_{en}) \quad (2)$$

In Eq. (2), individual expressions represent:  $h_F(\bar{T}_p - T_F)$  – heat flux flowing from the liquid porous material to the solidified layer, where the heat transfer coefficient on the solidification front surface is denoted by  $h_F$ , whereas  $\bar{T}_p(t)$  is the mean superheating temperature determined as a function of time. In the same equation  $\varphi \rho_S L d\delta/dt$  is the heat flux generated as a result of water solidification, where  $\rho_S$  is the density of ice,  $L$  it is the heat of solidification of water,  $d\delta/dt$  is the water solidification velocity, and  $t$  is solidification time. Further,  $(k_{sp}/\delta)(T_F - T_W)$  is the heat flux flowing through the solidified layer, where  $k_{sp}$  is the thermal conductivity of the solidified porous material;  $h_{en}(T_W - T_{en})$  is the heat flux flowing from the outer surface of the slab to the surroundings, and  $h_{en}$  is the heat transfer coefficient on the surface of the slab.

The quasi-steady-state heat balance Eq. (2) describes, in a quite accurate manner, the actual phenomenon of water solidification in a porous slab for the small Stefan numbers occurring in the studied phenomenon:  $Ste = \frac{c_S(T_F - T_{en})}{L} \ll 1$ , where  $c_S$  is the specific heat of ice.

In the first position variant (case “a”) the non-insulated surface is the bottom surface of the slab, while in the second (case “b”) the uninsulated surface is facing up. In both cases, the initial temperature of the porous medium of the slab is the same within the entire slab –  $T_{p0} = 293 \text{ K}$ . During solidification, the temperature distribution in the slab showed unevenness  $T_F < T_p(t) < T_{p0}$ . The location of the  $T_a \bar{H}(t)$  isotherm depends on the duration of the solidification process and marks the area of a fluid-saturated porous medium, in which the temperature is lower than the temperature of the water anomaly and greater than the freezing point –  $T_F < T_p < T_a$ . In the remaining part of the slab, the temperature of the fluid-saturated porous medium is higher. Water anomaly temperature and the solidification/freezing temperature are  $T_a \approx 277 \text{ K}$  and  $T_F = 273 \text{ K}$ , respectively.

Case “a” (Pure heat conduction in the fluid-saturated porous layer)

The temperature distribution in the steady-state superheated

fluid-saturated porous layer and the heat flux on the solidification surface.

Starting from the Fourier law in the following space:  $\delta \leq z < H$  (see Figure 1(a)) for the selected moment:

$$\frac{d^2 T}{dz^2} = 0, \quad (3)$$

with boundary conditions:

$$1^\circ \text{ for } z = \delta, T = T_F \quad (4)$$

$$2^\circ \bar{T}_p - T_F = \frac{\int_\delta^H (T - T_F) dz}{H - \delta} \quad (5)$$

which are described by the equation:

$$T(z, \delta) = \frac{2(\bar{T}_p - T_F)}{H - \delta} (z - \delta) + T_F, \quad (6)$$

and the heat flux on the solidification surface equals:

$$\dot{q} = k_{ef} \frac{\partial T}{\partial z} \Big|_{z=\delta} = 2k_{ef} \frac{T_p - T_F}{H - \delta} \quad (7)$$

By comparing the heat transferred and conducted on the liquid’s surface, the heat transfer coefficient  $h_F$  was obtained:

$$\dot{q} = h_F(\bar{T}_p - T_F) = 2 \frac{k_{ef}}{H - \delta} (\bar{T}_p - T_F) \rightarrow h_F = 2 \frac{k_{ef}}{H - \delta} \quad (8)$$

The average temperature of the porous fluid-saturated slab in the variable volume  $(H - \delta)$ , it is the same as boundary condition (5), is described by the equation:

$$\bar{T}_p - T_F = \frac{\int_\delta^H (T - T_F) dz}{H - \delta} \quad (9)$$

Change in capacitive heat in a fluid-saturated porous medium is described by the following equation:

$$\rho_{ef} c_{ef} \frac{d}{dt} \int_\delta^H (T - T_F) dz = \rho_{ef} c_{ef} \frac{d}{dt} [(\bar{T}_p - T_F)(H - \delta)] \quad (10)$$

From the heat balance equation for a liquid porous medium (the heat acquired from the liquid porous medium is equal to the heat of accumulation of the liquid porous medium), it follows that:

$$h_F(\bar{T}_p - T_F) = -\rho_{ef} c_{ef} \frac{d}{dt} [(\bar{T}_p - T_F)(H - \delta)]. \quad (11)$$

By transforming the Eqs. (1), (7), (8), (9), (10), the system of conjugated differential equations involving two unknowns  $\bar{\delta}, \bar{\theta}_p$  was obtained in a dimensionless form:

$$\begin{aligned} \frac{2\tilde{k}_{ef}}{1-\bar{\delta}} \bar{\theta}_p B + \varphi \tilde{k}_s \frac{d\bar{\delta}}{d\tau} &= \frac{Bi_{en}}{1+Bi_{en}\bar{\delta}} \\ \frac{2}{1-\bar{\delta}} \bar{\theta}_p &= -\kappa_s Ste \frac{d}{d\tau} [\bar{\theta}_p(1-\bar{\delta})] \end{aligned} \quad (12)$$

where:

$$\begin{aligned} \bar{\delta} &= \frac{\delta}{H}, \tau = Ste \cdot Fo, Ste = \frac{c_s(T_F - T_{en})}{L}, \bar{\theta}_p(\tau) = \frac{\bar{T}_p(\tau) - T_F}{T_{p0} - T_F}, Fo = \\ &= \frac{\kappa_s t}{H^2}, B = \frac{T_{p0} - T_F}{T_F - T_{en}}, Bi_{en} = \frac{H h_{en}}{\kappa_{sp}}, \tilde{k}_{ef} = \frac{k_{ef}}{\kappa_{sp}}, \tilde{k}_s = \frac{\kappa_s}{\kappa_{sp}}, \tilde{\kappa}_s = \frac{\kappa_s}{\kappa_{ef}}, \end{aligned}$$

which meet the initial condition:

$$\tau = 0, \bar{\delta} = 0 \text{ i } \bar{\theta}_p = 1 \quad (13)$$

Case “b”

In the case under consideration, free convection may occur in the fluid-saturated porous medium (see Figure 1(b)) and therefore the heat transfer coefficient  $h_F$  on the solidification surface requires different calculations to be performed. Using the Eqs. (2) and (11), the system of equations describing the above-mentioned phenomenon takes the form of:

$$\begin{aligned} BiB\bar{\theta}_p + \varphi \tilde{k}_s \frac{d\bar{\delta}}{d\tau} &= \frac{Bi_{en}}{1+Bi_{en}\bar{\delta}} \\ Bi\bar{\theta}_p &= -\tilde{\kappa}_s \tilde{k}_{ef} Ste \frac{d}{d\tau} [\bar{\theta}_p(1-\bar{\delta})], \end{aligned} \quad (14)$$

where,  $Bi \frac{h_F H}{\kappa_{sp}}$  is the Biot number on the solidification surface and  $\tilde{k}_{ef} = \frac{k_{ef}}{\kappa_{sp}}$ . The system of Eq. (14) satisfies the same initial condition (13) as in the instance of the case “a”. The Biot number on the solidification surface depends on the heat transfer coefficient on this surface and the free convection (Rayleigh number), however indirectly.

The theoretical models developed in this paper present the solidification equations of the moist porous medium (12, 14) are similar to the previous work of the authors for the solidification of a single-component medium [40].

### 3.2 Free convection

Free convection in the sub-areas of a fluid-saturated slab depending on its orientation. The heat flow through the fluid-saturated porous layer actually changes as the cooling process continues. An analysis of the heat flow in the fluid-saturated region of the slab, in two different position variants, is presented below.

Case “a”

In this case, free convection is possible in the lower part of the porous fluid-saturated slab (see Figure 1 (a)), when the Rayleigh number  $\tilde{R}a(t)$  in the initial stage of solidification, it meets the following condition (17):

$$\tilde{R}a(t) = \frac{Kg\beta(T_a - T_F)(\bar{H} - \delta)}{\nu\kappa_{ef}} > 40 \quad (15)$$

At the beginning of solidification, from the equation based on the work by Kimura et al. [16], Partyka and Lipnicki [25]

which determine the Rayleigh number, the minimum height of the fluid-saturated sublayer  $\bar{H}$  where free convection of the liquid may occur was calculated:

$$\tilde{R}a(t) = \Lambda \bar{H} \rightarrow \bar{H} > \frac{40}{\Lambda}, \quad (16)$$

The parameter extracted presented in the Eq. (15), which is independent of the external dimensions of the slab, is described by the equation:

$$\Lambda = \frac{Kg\beta(T_a - T_F)}{\nu\kappa_{ef}} \quad (17)$$

For a slab with a porous medium permeability  $K = 1.97 \cdot 10^{-8} m^2$  ( $\varphi = 0.50$ ) parameter  $\Lambda$  equals:

$$\Lambda = \frac{Kg\beta(T_a - T_F)}{\nu\kappa_{ef}} = \frac{1.97 \cdot 10^{-8} \cdot 9.81 \cdot 3.4 \cdot 10^{-5} \cdot (3.98 - 0)}{1.61 \cdot 10^{-6} \cdot 3.38 \cdot 10^{-7}} = 48.1 \frac{1}{m},$$

and the corresponding height of the sublayer in which free convection would occur should satisfy the following inequality:

$$\bar{H} > \frac{40}{\Lambda} = \frac{40}{48.1} = 0.832 \text{ m.}$$

The obtained calculations show that free convection can take place only for slabs whose thickness equals  $H > \bar{H} > 0.832 \text{ m}$ .

In the case under consideration, free convection does not appear in a layer with a thickness of  $H=0.5 \text{ m}$ , and the slab is positioned as in case “a”. Only heat conduction is possible. Similar results were obtained for the other two porous slabs ( $\varphi=0.54, \varphi=0.58$ ).

Case “b”

In this particular case, free convection is possible in the lower part of the porous fluid-saturated slab (see Figure 1(b)), if in the space under consideration ( $H - \bar{H} - \delta$ ) Rayleigh number  $\tilde{R}a(t)$  fulfils the following condition in the solidification phase:

$$\tilde{R}a(t) = \frac{Kg\beta(T_{p0} - T_a)(H - \bar{H} - \delta)}{\nu\kappa_{ef}} = \Lambda \cdot (H - \bar{H} - \delta) > 40. \quad (18)$$

Parameter  $\Lambda$  is independent of the thickness of the saturated porous layer and it equals:

$$\Lambda = \frac{Kg\beta(T_{p0} - T_a)}{\nu\kappa_{ef}} = \frac{1.97 \cdot 10^{-8} \cdot 9.81 \cdot 8.5 \cdot 10^{-5} \cdot (293 - 277)}{1.30 \cdot 10^{-6} \cdot 3.38 \cdot 10^{-7}} = 599 \frac{1}{m}, \quad (19)$$

and the height of the slab sublayer at the onset of solidification  $\delta=0$ , in which free convection takes place, should meet the condition resulting from Eq. (18):

$$H - \bar{H} > \frac{40}{\Lambda} \rightarrow \bar{H} < H - \frac{40}{\Lambda}. \quad (20)$$

The comparison of heat fluxes on an isothermal surface  $T = T_a$  is shown in the equation:

$$h_a \cdot (T_{p0} - T_a) = \frac{k_{ef}}{\bar{H}} (T_a - T_F), \quad (21)$$

where,  $h_a$  is the heat transfer coefficient from the side of the slab where free convection occurs. By transforming the Eq. (21) and using the relationship (18), the authors obtained an equation determining the heat transfer coefficient:

$$h_a = \frac{Nu \cdot k_L}{H - \tilde{H}} = \frac{\tilde{Ra} \cdot k_L}{40 \cdot H - \tilde{H}} = \frac{\Lambda(H - \tilde{H}) \cdot k_L}{40 \cdot H - \tilde{H}} = \frac{\Lambda k_L}{40} \quad (22)$$

Height  $\tilde{H}$  heat transfer coefficient on the solidification surface  $h_F$  and the Biot number  $Bi$ , are respectively equal to:

$$\tilde{H} = \frac{40k_{ef}(T_a - T_F)}{\Lambda k_L (T_{P0} - T_a)}, h_F = \frac{k_{ef}}{\tilde{H}}, Bi = \frac{h_F H}{k_{sp}} \quad (23)$$

The parameters calculated according to equations (8-23) and related to the case “b” are presented in Table 1.

In Table 1, the discussed parameters point to the existence of free convection in the fluid-saturated porous layer under consideration. The remaining Tables 2 and 3 list the calculated thermodynamic parameters of the porous matrix material, both the fluid-saturated and solidified porous bed for the porous layer prior to the solidification and following the solidification.

Table 4 shows the dimensionless parameters describing fluid-saturated and solidified porous slabs, depending on the porosity of the bed. This paper also presents the parameters determining the phenomenon within a fluid-saturated porous bed, namely:  $Ste$ ,  $Bi_{en}$ ,  $\tilde{Ra}$ ,  $Bi$ . Those parameters are used in the numerical calculations of the systems of Eqs. (12) and (14).

The presented results show that the Rayleigh number decreases with the increase in porosity. It should also be added that the condition for the occurrence of free convection for a

flat, unconfined horizontal layer is to exceed the critical number. The values of the critical Rayleigh Number for a flat porous layer limited by a vertical cylindrical wall are higher. This means that the adiabatic walls limiting the moist porous medium have a stabilizing effect on the flow occurring in it. The stabilizing effect of heat-conducting walls is even greater. Moreover, the critical Rayleigh number depends on the geometric parameter of the layer, the ratio of the layer's radius to its height. As the value of this parameter decreases, the critical Rayleigh number increases. However, as the Rayleigh number increases, the intensity of liquid flow in the unsolidified part of the porous medium increases, which results from the work of Bejan [37].

### 3.3 Theoretical research results

To find a numerical solution to the system of Eqs. (12)-(14) with the initial conditions (13), a suitable program was developed within MATLAB software. Numerical results of the solution of the system of Eqs. (12)-(14) are presented in Figures 2-6. These results were selected here to illustrate their dependence of several dimensionless parameters.

Figure 2 shows the course of the average superheat temperature  $\bar{\theta}_p$  and the thickness of the solidified layer  $\tilde{\delta}$ , for the case “a”, depending on the time  $\tau$ . The case “a” (see Figure 1(a)) describes the solidification of a fluid-saturated porous slab in the absence of free convection and when the superheating parameter  $B=2$  ( $T_{P0}=293$  K,  $T_{en}=263$  K). The average superheating temperature of the fluid-saturated porous slab decreases with time, while the thickness of the solidified layer rises.

**Table 1.** Parameters describing free convection in a fluid-saturated porous layer and on the surface of the solidification front for the case “b”

$\varphi$	$\Lambda, 1/m$	$\tilde{H}, m$	$\tilde{H}, m$	$h_a, W/(m^2K)$	$h_F, W/(m^2K)$	$Bi$
0.50	599	< 0.433	0.0215	8.69	34.9	12.0
0.54	531	< 0.425	0.0238	7.70	31.0	10.4
0.58	514	< 0.422	0.0242	7.45	30.0	9.74

**Table 2.** Fluid-saturated bed parameters

$c_k$	$\rho_k$	$k_k$	$\kappa_k$	$c_L$	$\rho_L$	$k_L$	$\kappa_L$	$\varphi$	$c_{ef}$	$\rho_{ef}$	$k_{ef}$	$\kappa_{ef}$
$\frac{J}{kgK}$	$\frac{kg}{m^3}$	$\frac{W}{mK}$	$\frac{m^2}{s}$	$\frac{J}{kgK}$	$\frac{kg}{m^3}$	$\frac{W}{mK}$	$\frac{m^2}{s}$	%	$\frac{J}{kgK}$	$\frac{kg}{m^3}$	$\frac{W}{mK}$	$\frac{m^2}{s}$
1130	1800	0.900	$4.42 \cdot 10^{-7}$	4200	1000	0.580	$1.43 \cdot 10^{-7}$	50	1872	1187	0.751	$3.38 \cdot 10^{-7}$
								54	1735	1263	0.738	$3.37 \cdot 10^{-7}$
								58	1645	1345	0.726	$3.28 \cdot 10^{-7}$

**Table 3.** Solidified bed parameters

$c_k$	$\rho_k$	$k_k$	$\kappa_k$	$c_L$	$\rho_L$	$k_L$	$\kappa_L$	$\varphi$	$c_{ef}$	$\rho_{ef}$	$k_{ef}$	$\kappa_{ef}$
$\frac{J}{kgK}$	$\frac{kg}{m^3}$	$\frac{W}{mK}$	$\frac{m^2}{s}$	$\frac{J}{kgK}$	$\frac{kg}{m^3}$	$\frac{W}{mK}$	$\frac{m^2}{s}$	%	$\frac{J}{kgK}$	$\frac{kg}{m^3}$	$\frac{W}{mK}$	$\frac{m^2}{s}$
1130	1800	0.900	$4.42 \cdot 10^{-7}$	2135.0	917.0	2.0	$1.43 \cdot 10^{-7}$	50	1375	1125	1.45	$9.37 \cdot 10^{-7}$
								54	1330	1209	1.49	$9.27 \cdot 10^{-7}$
								58	1300	1299	1.54	$9.12 \cdot 10^{-7}$

**Table 4.** Dimensionless parameters in Eqs. (12) and (14)

$\varphi$	$\tilde{k}_{ef}$	$\tilde{k}_s$	$\tilde{\kappa}_s$	$Ste$	$Bi_{en}$	$Ra(0)$	$Bi$
0.50	0.518	1.379	0.423	0.064	3.45	287	12.0
0.54	0.495	1.339	0.424	0.064	3.36	253	10.4
0.58	0.471	1.300	0.436	0.064	3.25	245	9.74

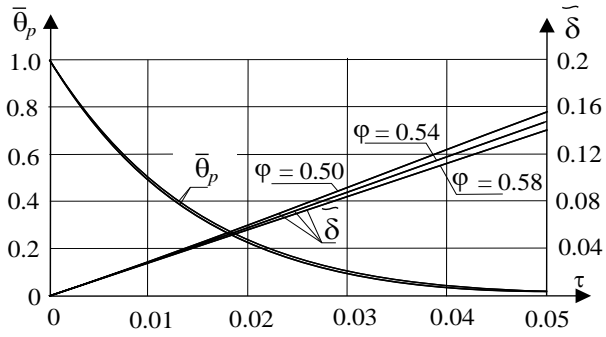


**Figure 2.** Dependence of average superheating temperature and the thickness of the solidified layer on time, no free convection (case “a”),  $B=2$

The impact of porosity  $\phi$  is clear in the curves representing the thickness of the solidified layers. Out of all the porosities tested, the greatest increase in the thickness of the solidified layer was observed for  $\phi=0.50$ . However, the temperature distributions for these porosities differ only slightly, and they practically form one single curve.

The influence of water free convection on temperature courses  $\bar{\theta}_p$  and the thickness of the solidified layer  $\bar{\delta}$  in a fluid-saturated porous slab can be read in Figure 3. This is case “b” (see Figure 1(b)). At the beginning of the process  $\tau=0$  and no increase in the thickness of the solidified layer was observed, which stems from the theoretical model of the solidification phenomenon. At the onset of the process, the derivative of the layer thickness versus time  $\frac{d\bar{\delta}}{d\tau}$  (solidification velocity) for the following parameters:  $Bi_{en} = 3.45, B = 2, Bi = 12, \phi = 0.5, \tilde{k}_s = 1.38$  assumed negative value and it equalled:

$$\frac{d\bar{\delta}}{d\tau}(0) = \frac{Bi_{en} - Bi B}{\phi \tilde{k}_s} = -29.8 < 0, \quad (24)$$

which meant that the solidification of the liquid did not occur. The unrealistic course of the solidified layer thickness is shown in Figure 3 with a dashed line. For case “b”, what appears from the solidification plot (see Figure 3 and Figure 5), is that the onset of solidification occurs at approximately  $\tau \approx 0.008$  ( $\frac{d\bar{\delta}}{d\tau(\tau)} > 0, \bar{\delta} = 0$ ). As a result of the free convection of the liquid, the cooling process begins in the time interval  $0 < \tau < 0.008$ : the amount of heat supplied to the potential solidification zone of the porous slab from the warm part of the porous medium slab is still relatively large, and that prevents the fluid from solidifying in the overall heat balance.

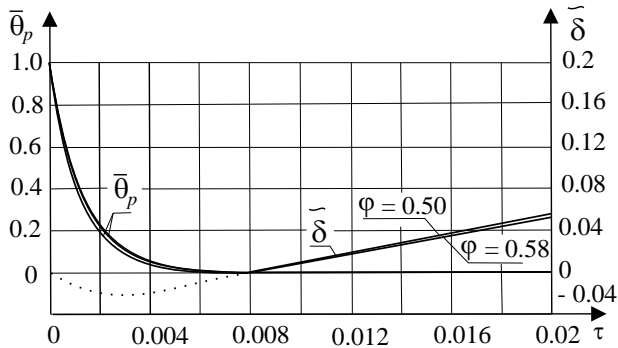


**Figure 3.** Dependence of average superheating temperature and the thickness of the solidified layer on time, presence of free convection (case “b”),  $B=2$

Indeed, as the slab cools down, the amount of heat supplied decreases and conditions conducive to the solidification process occur. In fact, free convection vanishes – Rayleigh number  $Ra(t)$  decreases, which in the theoretical model is assumed to be constant and equal to the initial Rayleigh number  $Ra(0)$ . It is a kind of permissible simplification of this physical phenomenon.

For case “b”, the average superheating temperature of a fluid-saturated porous slab decreases much faster due to the existence of free convection (the liquid is mixed) than in case “a” for which only heat conduction occurs (see Figures 2 and 3).

Figures 4, 5 and 6 illustrate the growth of the solidification layer for various superheating parameters:  $B = 0$  ( $T_{p0} = T_F$ ),  $B = 2$  ( $T_{p0} = 293 K, T_{en} = 263 K$ ) and  $B = 0.5$  ( $T_{p0} = 293 K, T_{en} = 233 K$ ).

As the superheating parameter increases, the fluid-saturated porous slab solidification rate decreases. The impact of the superheat parameter on the solidification process is quite substantive.

As can be seen from the theoretical model tests presented in Figure 7, the positioning of the fluid-saturated porous slab clearly affects its solidification rates in the initial solidification stage. In case “b”, the positioning of the slab promotes the formation of free convection of water, which delays, as previously discussed, the onset of solidification. For longer times, the two solidification curves coincide. By recalculating dimensionless time into dimensional time, what could be seen is that initially, the phenomenon lasts for quite a long time. For the analysed superheating parameter  $B=2$ , e.g. for the dimensionless time  $\tau=0.02$  the corresponding real-time is  $\approx 49$  hours. For case “a” the solidification is more intense than for case “b” within the discussed dimensionless time.

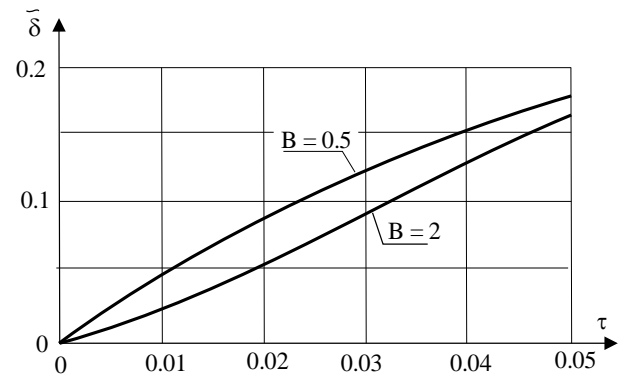


**Figure 4.** Comparison of the growth of solidified layer for two superheating and case “a”

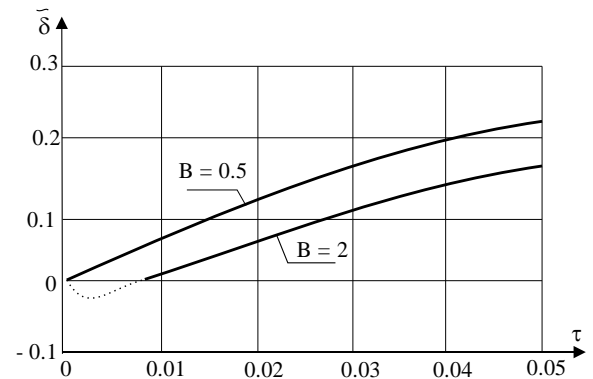


**Figure 5.** Comparison of the growth of solidified layer for two superheating parameters and case “b”

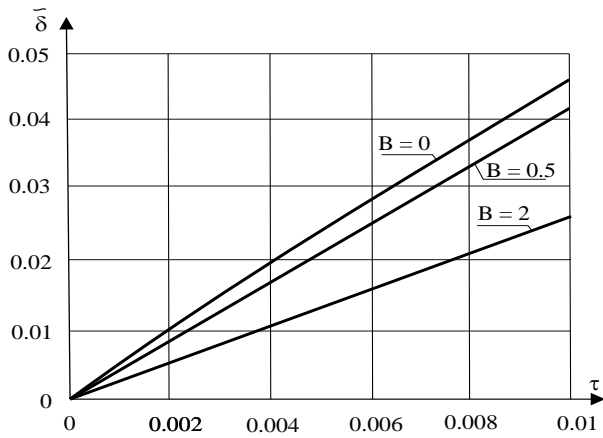


**Figure 6.** Solidification of a fluid-saturated porous slab for various superheating parameters and porosity  $\varphi=0.50$  (case "a")

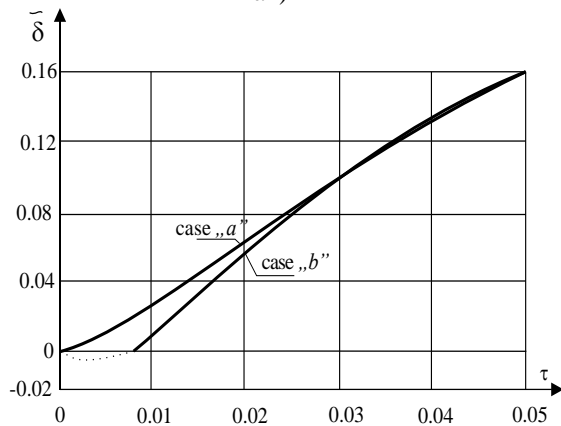


**Figure 7.** Comparison of solidification for two fluid-saturated porous slab positions for superheating parameters  $B=2$  and porosity  $\varphi=0.50$

It should be stated that the simple theoretical model proposed in this work is considered in two cases, to describe the phenomenon of water solidification occurring in layers of a porous medium limited by flat surfaces at different temperatures, is justified, sufficient and provides practical benefits. The adoption of the heat transfer coefficient  $h_F$  on the surface of the solidification front is justified in the theoretical analysis of the phenomenon of solidification in humid porous media, because it influences the course of solidification. This, in turn, is of great practical importance due to the technical condition of structural elements of buildings and structures, as well as the implementation of preventive measures as part of effective frost protection.

## 4. EXPERIMENTAL TESTS

### 4.1 General characteristics of the elements of the test stand

In order to verify the theoretical solutions to the problem of solidification in a planar fluid-saturated porous layer, experimental studies of fluid-saturated granular media were carried out on the test stand designed and constructed by the authors, which is shown in Figures 8, 9 and 10.

The test stand, which is characterised by a universal design was also used for this study of water solidification in other porous media [25].

The main element of the test stand is a chamber made of

polymethyl methacrylate (PMMA) with an internal diameter of 6.4 cm and a height of 25 cm. In the experiment, it was possible to use mainly the property of the material that concerns high transparency and transparency, of the order of 98%, which made it possible to visualize the course of the phenomenon under appropriate conditions of the experiment. Other properties of the central unit material that are valuable for research include a minimum operating temperature of  $-40^{\circ}\text{C}$  and a maximum of  $+70^{\circ}\text{C}$ , high hardness according to the Rockwell scale, dimensional stability up to  $102^{\circ}\text{C}$  and resistance to most chemical products.



**Figure 8.** Test stand

The test chamber was placed vertically. In its lower and upper parts, the chamber is enclosed with covers with a collar made of plexiglass and connected with combination screws. A hole was made in the wall of the chamber, in which a valve was inserted to equalize the pressure caused by the increase in the volume of ice formed by the water freezing. The porous granular bed shown in Figure 9 is a mixture of washed river gravel with a grain diameter of 2-16 mm. The decisive factor in selecting the aggregate for testing was the versatility of its use in the construction industry. It is used for products in the form of slabs, as well as the production of various types of concretes and mortars.



**Figure 9.** A porous granular bed filling the test chamber

In the lower part of the test chamber, the porous bed is adjacent to the copper slab, and the ribbings on its surface increase the efficiency of heat removal, resulting from the solidification process within the porous bed. Ethylene glycol was selected as the circulating coolant.

The temperature was measured with the use of five Pt 100 resistance thermometers connected to a multi-channel data recorder. The thermometers have been arranged with the first temperature sensor being mounted at a distance of 0.5 cm from the copper cooling slab, while the others, equidistant from each other, are spaced 1 cm apart.

A limited number of sensors were used in the experiment in order to minimize the expected flow disturbances, and the selection and type of sensors were determined by criteria such as their low chemical activity, relatively long sensor operation time, wide temperature measurement range, stability of the time function and almost linear characteristics of the temperature coefficient resistance throughout the entire operating temperature range. The sensors were connected to the AR 207 data recorder from APAR.

The diagram of the test chamber is shown in Figure 10.

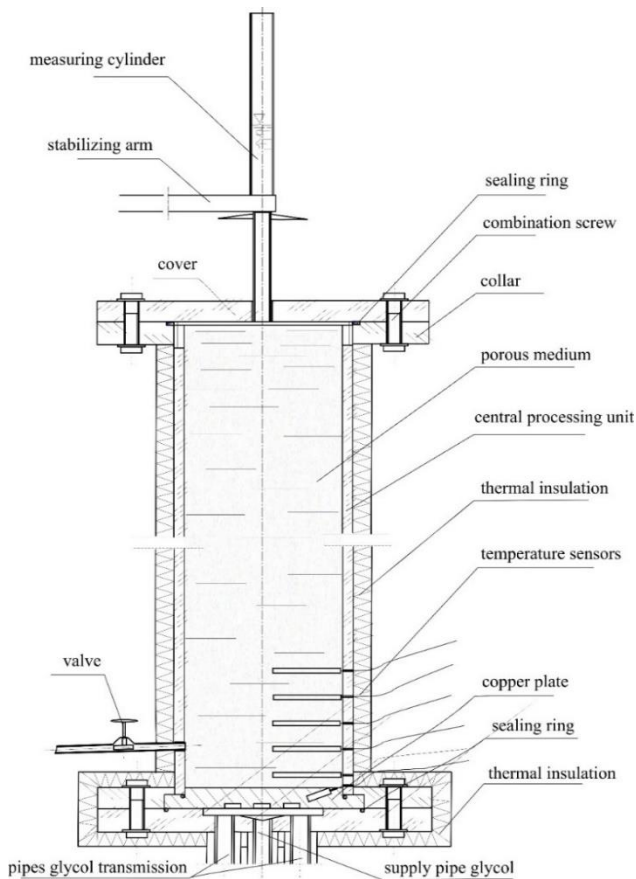


Figure 10. Diagram of the test chamber [25]

An important element of the central unit is a flexible conduit placed in the upper cover and flange, connected to a measuring cylinder, which was used to measure the volume of water displaced from the freezing porous material in order to determine the thickness of the solidified layer being formed. The entire research stand ensured mobility and easy connection to the unit's power source and glycol supply and discharge. To obtain a better visualization effect of the experiment, it was also possible to illuminate the central unit, thanks to which the solidification process taking place in the porous medium could be observed on an ongoing basis.

#### 4.2 Research assumptions and criteria as well as the adopted experimental methodology

The basic assumptions and research criteria resulted from

the comparative analysis of other experiments conducted by the authors and theoretical models we developed and described by Beckermann and Viskanta [41], Sasaki et al. [42], and Banaszek et al. [43], among others.

In research on the solidification process of porous materials, the gravimetric (dryer) method was used to dry the granular material before the experiment and measure its mass loss. In addition, other methods were also used in the experiment, namely graduated cylinder, in which the solidification front was determined indirectly by measuring the increase in water volume in the graduated cylinder connected to the central unit and optical, related to the current assessment of the thickness of the solidified layer.

Before starting the experiment, preparatory activities were carried out each time, which included filling a measuring cylinder with water at a specific temperature to the initial scale, setting up and operating measuring instruments while observing the solidification process taking place in the porous bed and recording changes in the temperature in the bed, air temperature, glycol, copper plate in the central unit and ultrathermostat, increase in water volume in the measuring cylinder and fluctuations in the filling levels of piezometers with glycol.

The average thickness of the solidified layer was determined similarly as in the works of Lipnicki and Weigand [19], Partyka and Lipnicki [25].

#### 4.3 Results and discussion

The proposed and adopted simple theoretical model to describe the phenomenon of free convection (or heat conduction) and solidification occurring in layers of a porous medium bounded by flat surfaces at different temperatures is sufficiently accurate and provides practical benefits.

The development of the solidification front over time and its impact on free convection in a moist porous medium located in the field of gravity is insignificant.

The presented method of determining the heat transfer coefficient  $h_f$  on the surface of the solidification front provides computational advantages.

As a result of the experimental measurements, the obtained results of the solidified layer thickness and temperature at the indicated points of the porous slab with porosity  $\phi=0.50$  above the surface of the cooling slab  $H$  as a function of time are shown in Figures 11 and 12.

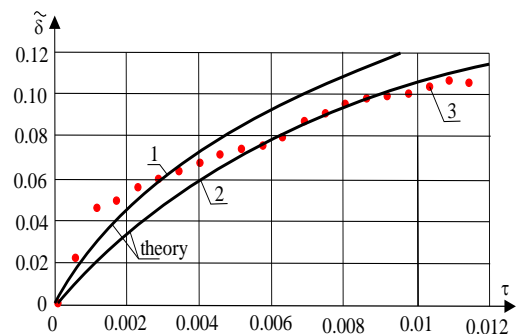
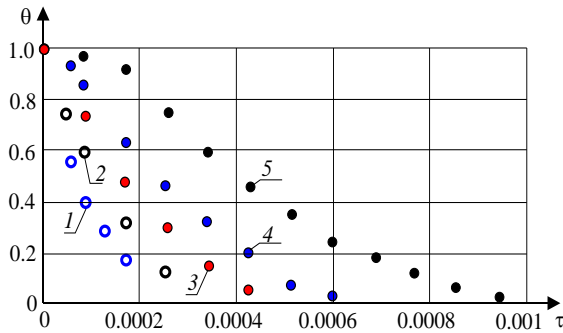


Figure 11. Thickness of the solidified layer as a function of time for the slab surface temp: 1-B=0;  $Bi_G=20$ , 2-B=2.5;  $Bi_G=20$ ; 3-B=2.5;  $Bi_G=20$  (experiment)

The results of theoretical research on the solidification of fluid-saturated porous layers with no free convection can be compared with the experimental tests performed on the test



stand, as its design ensures that heat is conducted through the porous layer without the occurrence of free convection.



**Figure 12.** Temperature distribution in the porous layer for  $T_w=263$  K,  $H=$ : 1-5 mm, 2-15 mm, 3-25 mm, 4-35 mm, 5- 45 mm

From the graphs of experimental studies shown in Figures 11 and 12 it can be seen that at the beginning of the solidification process, the solidification velocity (increase in the thickness of the solidified layer) is relatively high. The greatest thickness of the solidified layer was noted for porosity  $\varphi=0.50$  (see Figure 11). Temperatures inside the fluid-saturated porous layer at the marked points and at the distance  $H$  from the lower cooling slab, decrease as the process  $\tau$  progresses (see Figure 12).

The calculations, in accordance with the developed theoretical model, were compared with the experimental tests for the conditions of intensive cooling, i.e.  $Bi_{en} = Bi_G = 20$ . Figure 11 shows the theoretical solidification lines of a non-superheated liquid ( $B=0$ ) line - 1, superheated liquid ( $B=2.5$ ) line - 2 and experimental measuring points - 3. As can be seen the results of experimental tests on the thickness of the solidified layer, carried out under the conditions laboratory tests, are consistent with the results obtained according to the theoretical model proposed in this paper. In the initial stage of solidification, the experimental points differ the most from the theoretical line marked with the number 2, the reason for this may be a temporary increase, during the experimental measurements, of the Biot number  $Bi_G$ .

Moreover, it should be stated that the developed simplified theoretical model of the coagulation phenomenon is satisfactorily consistent with experimental research, and the design of the new test stand to conduct this research is an innovative solution, based on an original research concept.

## 5. CONCLUSIONS

The most important achievements of the work include the development of simple analytical theoretical models describing the solidification processes, the solution and analysis of which allow to describe qualitatively and quantitatively the phenomenon of solidification of horizontal wet porous slabs.

One of the most important benefits resulting from this work is the development of an interesting research concept for understanding the solidification process taking place in moist porous media. The design of the research stand for testing the coagulation process is a new solution, based on an individual concept.

It is possible to use temperature measurement sensors with a smaller diameter, which will reduce the negative impact of

the disturbances on the solidification process, mainly caused by holes made in the wall with sensors inserted.

The main characteristics of the model include the adoption and calculation of the heat transfer coefficient at the solidification front depending on the slab setting. The theoretical research carried out shows the impact of the positioning of the horizontal fluid-saturated porous slab relative to the force of gravity on the formation of free convection in the fluid-saturated porous layer and, indirectly, on the solidification process itself.

Due to the existence of free convection, the solidification process starts later for the "b" case, than for the "a" case. The onset of solidification is relatively long (for the case under consideration it took about two days) and it progresses during this period noticeably. The solidification rate is significantly impacted by the  $B$  superheating parameter and with the increase of this parameter, the solidification rate for the fluid-saturated porous slab decreases. The results of the experimental research are largely in agreement with the results of the theoretical research. The lower quantitative compatibility of the theoretical and experimental results from different external cooling conditions adopted in the theoretical model when compared with those in laboratory tests.

The experimental tests in laboratory conditions that would fully comply with the theoretical model were not conducted, however, there are plans to modify the test stand in the future will, which would allow for completely accurate verification of the theoretical model.

The problem of water coagulation in porous media is of great scientific and technical importance, the observations and comments presented above regarding the problem of water coagulation in moist porous materials, indicate a constant need for further research on this complex physical process, which is of fundamental importance for engineering.

## REFERENCES

- [1] Weaver, J.A., Viskanta, R. (1986). Freezing of water saturated porous media in a rectangular cavity. *International Communications in Heat and Mass Transfer*, 13(3): 245-252. [https://doi.org/10.1016/0735-1933\(86\)90013-8](https://doi.org/10.1016/0735-1933(86)90013-8)
- [2] Sasaki, A., Aiba, S., Fukusako, S. (1990). Numerical study on freezing heat transfer in water-saturated porous media. *Numerical Heat Transfer*, 18(1): 17-32. <https://doi.org/10.1080/10407789008944781>
- [3] Banerjee, T., Chang, C., Wu, W., Narusawa, U. (1992). Solidification with a throughflow in a porous medium. *ASME Journal of Heat and Mass Transfer*, 114(3): 675-680. <https://doi.org/10.1115/1.2911333>
- [4] Matsumoto, K., Okada, M., Murakami, M., Yabushita, Y. (1993). Solidification of porous medium saturated with aqueous solution in a rectangular cell. *International Journal of Heat and Mass Transfer*, 36(11): 2869-2880. [https://doi.org/10.1016/0017-9310\(93\)90106-G](https://doi.org/10.1016/0017-9310(93)90106-G)
- [5] Song, M., Choi, J., Viskanta, R. (1993). Upward solidification of a binary solution saturated porous medium. *International Journal of Heat and Mass Transfer*, 36(15): 3687-3695. [https://doi.org/10.1016/0017-9310\(93\)90048-B](https://doi.org/10.1016/0017-9310(93)90048-B)
- [6] Gawin, D., Schrefler, B.A., Galindo, M. (1996). Thermo-hydro-mechanical analysis of partially saturated porous materials. *Engineering Computations*, 13(7): 113-143. <https://doi.org/10.1108/02644409610151584>

- [7] Nasser, I., Duwairi, H.M. (2016). Thermal dispersion effects on convection heat transfer in porous media with viscous dissipation. *International Journal of Heat and Technology*, 34(2): 207-212. <https://doi.org/10.18280/ijht.340208>
- [8] Nithiarasu, P., Seetharamu, K.N., Sundararajan, T. (1998). Effect of porosity on natural convective heat transfer in a fluid saturated porous medium. *International Journal of Heat and Fluid Flow*, 19(1): 56-58. [https://doi.org/10.1016/S0142-727X\(97\)10008-X](https://doi.org/10.1016/S0142-727X(97)10008-X)
- [9] Mackie, C., Desai, P., Meyers, C. (1999). Rayleigh-Bénard stability of a solidifying porous medium. *International Journal of Heat and Mass Transfer*, 42(17): 3337-3350. [https://doi.org/10.1016/S0017-9310\(98\)00361-5](https://doi.org/10.1016/S0017-9310(98)00361-5)
- [10] Geindreau, C., Auriault, J.L. (2001). Transport phenomena in saturated porous media undergoing liquid-solid phase change. *Archives of Mechanics*, 53(4-5): 385-420.
- [11] Hwang, I.G. (2001). Convective instability in porous media during solidification. *American Institute of Chemical Engineers. AIChE Journal*, 47(7): 1698.
- [12] Song, M., Viskanta, R. (2001). Lateral freezing of an anisotropic porous medium saturated with an aqueous salt solution. *International Journal of Heat and Mass Transfer*, 44(4): 733-751. [https://doi.org/10.1016/S0017-9310\(00\)00132-0](https://doi.org/10.1016/S0017-9310(00)00132-0)
- [13] Watanabe, K., Mizoguchi, M. (2002). Amount of unfrozen water in frozen porous media saturated with solution. *Cold Regions Science and Technology*, 34(2): 103-110. [https://doi.org/10.1016/S0165-232X\(01\)00063-5](https://doi.org/10.1016/S0165-232X(01)00063-5)
- [14] Rattanadecho, P. (2004). Experimental and numerical study of solidification process in unsaturated granular packed bed. *Journal of Thermophysics and Heat Transfer*, 18(1): 87-93. <https://doi.org/10.2514/1.9155>
- [15] Kimura, S., Okajima, A., Nihon Kikai Gakkai Ronbunshu, B. (2005). Experimental study of heat transfer in an open thermosyphon. *Transactions of the Japan Society of Mechanical Engineers, Part B*, (71): 931-938. <https://doi.org/10.1299/kikaib.71.931>
- [16] Kimura, S., Okajima, A., Kiwata, T., Fusaoka, T. (2006). Solidification in a water-saturated porous medium when convection is present (response of solid-liquid interface due to time-varying cooling temperature). *Heat Transfer-Asian Research: Co-sponsored by the Society of Chemical Engineers of Japan and the Heat Transfer Division of ASME*, 35(4): 294-308. <https://doi.org/10.1002/hjt.20109>
- [17] Le Bars, M., Worster, M.G. (2006). Interfacial conditions between a pure fluid and a porous medium: Implications for binary alloy solidification. *Journal of Fluid Mechanics*, 550: 149-173. <https://doi.org/10.1017/S0022112005007998>
- [18] Cheng, W.T., Lin, C.H. (2007). Melting effect on mixed convective heat transfer with aiding and opposing external flows from the vertical plate in a liquid-saturated porous medium. *International Journal of Heat and Mass Transfer*, 50(15-16): 3026-3034. <https://doi.org/10.1016/j.ijheatmasstransfer.2006.12.018>
- [19] Lipnicki, Z., Weigand, B. (2008). Natural convection flow with solidification between two vertical plates filled with a porous medium. *Heat and Mass Transfer*, 44: 1401-1407. <https://doi.org/10.1007/s00231-008-0368-6>
- [20] Vlahou, I., Worster, M.G. (2010). Ice growth in a spherical cavity of a porous medium. *Journal of Glaciology*, 56(196): 271-277. <https://doi.org/10.3189/002214310791968494>
- [21] Wei, P.S., Hsiao, S.Y. (2017). Effects of solidification rate on pore shape in solid. *International Journal of Thermal Sciences*, 115: 79-88. <https://doi.org/10.1016/j.ijthermalsci.2017.01.012>
- [22] Khongkaew, W., Sertikul, C., Rttandecho, P. (2018). Experimental and numerical study of the solidification process in saturated porous media: Influence of the solid particle, types and freezing temperature. *Songklanakarin Journal of Science and Technology*, 40(3): 623-632.
- [23] Kim, M.C. (2019). Onset of buoyancy-driven convection in a fluid-saturated porous layer bounded by semi-infinite coaxial cylinders. *Korean Chemical Engineering Research*, 57(5): 723-729. <https://doi.org/10.9713/kcer.2019.57.5.723>
- [24] Massarotti, N., Mauro, A., Trombetta, V. (2021). A general numerical procedure for solidification and melting in porous media and free fluids. *International Journal of Thermal Sciences*, 161: 106716. <https://doi.org/10.1016/j.ijthermalsci.2020.106716>
- [25] Partyka, J., Lipnicki, Z. (2018). Influence of external conditions on the solidification process in saturated porous planar layers, *International Journal of Heat and Mass Transfer*, 127: 75-83. <https://doi.org/10.1016/j.ijheatmasstransfer.2018.06.123>
- [26] Wang, M., Bejan, A. (1987). Heat transfer correlation for Bénard convection in a fluid saturated porous layer. *International Communications in Heat and Mass Transfer*, 14(6): 617-626. [https://doi.org/10.1016/0735-1933\(87\)90041-8](https://doi.org/10.1016/0735-1933(87)90041-8)
- [27] Seki, N., Fukusako, S., Sugawara, M. (1977). A criterion of onset of free convection in a horizontal melted water layer with free surface. *Journal of Heat Transfer*, 99: 92-98. <https://doi.org/10.1115/1.3450661>
- [28] Yen, Y.C. (1990). Natural convection heat transfer in water near its density maximum. *US Army Corps of Engineers, Cold Regions Research & Engineering Laboratory*.
- [29] Weaver, J.A., Viskanta, R. (1986). Melting of frozen, porous media contained in a horizontal or a vertical, cylindrical capsule. *International Journal of Heat and Mass Transfer*, 29(12): 1943-1951. [https://doi.org/10.1016/0017-9310\(86\)90013-X](https://doi.org/10.1016/0017-9310(86)90013-X)
- [30] Ng, K.W., Gong, Z.X., Mujumdar, A.S. (1998). Heat transfer in free convection-dominated melting of a phase change material in a horizontal annulus. *International communications in Heat and Mass Transfer*, 25(5): 631-640. [https://doi.org/10.1016/S0735-1933\(98\)00050-5](https://doi.org/10.1016/S0735-1933(98)00050-5)
- [31] Dzindziora, A., Cieřlik, J., Wojciechowski, J. (2021). Phase change materials and their use for energy accumulation. *MATEC Web of Conferences*, 338: 01006. <https://doi.org/10.1051/mateconf/202133801006>
- [32] Moeini Sedeh, M., Khodadadi, J.M. (2014). Solidification of phase change materials infiltrated in porous media in presence of voids. *Journal of Heat Transfer*, 136(11): 112603. <https://doi.org/10.1115/1.4028354>
- [33] Kenisarin, M.M., Mahkamov, K., Costa, S.C., Makhkamova, I. (2020). Melting and solidification of PCMs inside a spherical capsule: A critical review. *Journal of Energy Storage*, 27: 101082.

- <https://doi.org/10.1016/j.est.2019.101082>
- [34] Sobieski, W., Lipiński, S., Dudda, W., Trykozko, A., Marek, M., Wiącek, J., Matyka, M., Gołembiewski, J. (2016). Granular porous media (in English). Granularne ośrodki porowate (in Polish). Katedra Mechaniki i Podstaw Konstrukcji Maszyn, Olsztyn. [https://www.uwm.edu.pl/wpm/download/2016/wpm\\_2016\\_monografia.pdf](https://www.uwm.edu.pl/wpm/download/2016/wpm_2016_monografia.pdf).
- [35] Xu, W., Zhang, K., Zhang, Y., Jiang, J. (2022). Packing fraction, tortuosity, and permeability of granular-porous media with densely packed spheroidal particles: Monodisperse and polydisperse systems. *Water Resources Research*, 58(2): e2021WR031433. <https://doi.org/10.1029/2021WR031433>
- [36] Ismail, K.A.R., Pimentel, J.R. (1996). Analysis of the solidification process in porous saturated medium. In 2nd European Thermal-Sciences and 14th UIT National Heat Transfer Conference Rome, Italy, pp. 255-260. <http://doi.org/10.13140/2.1.1509.2000>
- [37] Bejan, A. (1984). *Convection Heat Transfer*. Wiley, New York.
- [38] Klemm, P. (2005-2008). *Praca zbiorowa: Budownictwo Ogólne, tom 2 Fizyka budowli*, Arkady, Warszawa (in Polish).
- [39] Zeng, Q., Li, K. (2019). Quasi-liquid layer on ice and its effect on the confined freezing of porous materials. *Crystals*, 9(5): 250. <https://doi.org/10.3390/cryst9050250>
- [40] Lipnicki, Z., Małolepszy, T. (2020). Analytical study of the solidification of a phase change material in an annular space. *Energies*, 13(21): 5561. <https://doi.org/10.3390/en13215561>
- [41] Beckermann, C., Viskanta, R. (1988). Natural convection solid/liquid phase change in porous media. *International Journal of Heat and Mass Transfer*, 31(1): 35-46. [https://doi.org/10.1016/0017-9310\(88\)90220-7](https://doi.org/10.1016/0017-9310(88)90220-7)
- [42] Sasaki, A., Aiba, S., Fukusako, S. (1992). Freezing heat transfer in water-saturated porous media in a vertical rectangular vessel. *Wärme-und Stoffübertragung*, 27(5): 289-298. <https://doi.org/10.1007/BF01589966>
- [43] Banaszek, J., Kowalewski, T.A., Furmański, P., Rebow, M., Cybulski, A., Wiśniewski, T.S. (2000). Konwekcja naturalna z przemianą fazową w układach jednoskładnikowych i binarnych. *Prace Instytutu Podstawowych Problemów Techniki PAN*, 3-125. <https://www.rcin.org.pl/publication/6249>.

## NOMENCLATURE

$c_k$	specific heat of grain, $J.kg^{-1}.K^{-1}$
$c_L$	specific heat of water, $J.kg^{-1}.K^{-1}$
$c_s$	specific heat of water, $J.kg^{-1}.K^{-1}$
$c_{ef}$	specific heat of moist porous medium, $J.kg^{-1}.K^{-1}$
$c_{sp}$	specific heat of frozen layer, $J.kg^{-1}.K^{-1}$
$h_f$	heat transfer coefficient on the solidification front, $W.m^{-2}.K^{-1}$
$h_{en}$	heat transfer coefficient on the surface slab, $W.m^{-2}.K^{-1}$

$k_k$	heat conductivity of aggregate, $W.m^{-1}.K^{-1}$
$k_L$	heat conductivity of water, $W.m^{-1}.K^{-1}$
$k_s$	heat conductivity of ice, $W.m^{-1}.K^{-1}$
$k_{ef}$	effective heat conductivity of the fluid-saturated porous medium, $W.m^{-1}.K^{-1}$
$k_{sp}$	heat conductivity of frozen layer, $W.m^{-1}.K^{-1}$
$t$	time of solidification, s
$H$	the thickness of a planar slab, m
$L$	latent heat of water, $J.kg^{-1}.K^{-1}$
$T_a$	water anomaly temperature, K
$T_{en}$	air temperature, K
$T_F$	solidification temperature, K
$T_{P0}$	the initial temperature of the porous medium of the slab, K
$T_w$	slab surface temperature, K

## Greek symbols

$\beta$	coefficient volumetric expansion of water, $K^{-1}$
$\rho_k$	grain density, $kg.m^{-3}$
$\rho_L$	water density, $kg.m^{-3}$
$\rho_s$	ice density, $kg.m^{-3}$
$\nu$	kinematic viscosity of water, $m^2.s^{-1}$
$\kappa_k$	thermal diffusion coefficient of the grain, $m^2.s^{-1}$
$\kappa_L$	thermal diffusion coefficient of the water, $m^2.s^{-1}$
$\kappa_s$	thermal diffusion coefficient of the solid, $m^2.s^{-1}$
$\kappa_{sp}$	thermal diffusion of frozen porous layer, $m^2.s^{-1}$
$\kappa_{ef}$	thermal diffusion coefficient of most porous medium, $m^2.s^{-1}$
$\varphi$	porosity of the medium, %
$\rho_{ef}$	density of most porous medium, $kg.m^{-3}$
$\rho_{sp}$	density of frozen layer, $kg.m^{-3}$
$\delta$	thickness of frozen layer, m

## Subscripts

$\tilde{\kappa}_{ef}$	ratio of the effective thermal conductivities of the fluid-saturated and frozen porous medium = $k_{ef}.k_{sp}^{-1}$
$\tilde{\kappa}_s$	ratio of the thermal diffusion of ice and the effective thermal diffusion of the fluid - saturated porous medium = $\kappa_s.k_{sp}^{-1}$
$\tilde{\kappa}_s$	ratio of the thermal diffusion of ice and the effective thermal diffusion of the fluid - saturated porous medium = $\kappa_s.\kappa_{ef}^{-1}$
$\tilde{\delta}$	dimensionless thickness of frozen layer = $\delta.H^{-1}$
$\tau$	dimensionless time = $Ste.F_0$
$Ste$	Stefan number = $c_s.(T_F - T_{en}).L^{-1}$
$Fo$	Fourier number
$Bi$	Biot number on the solidification front = $H.h_f.k_{sp}^{-1}$
$Bi_{en}$	Biot number on the surface of the slab = $H.h_{en}.k_{sp}^{-1}$
$B$	overheating parameter = $(T_{P0} - T_F).(T_F - T_{en})^{-1}$
$Ra$	Rayleigh number = $g\beta K\Delta TH.(\nu\kappa_L)^{-1}$